Nonlinear Coupled Tank System Control Using Optimal Evolutionary Neural Sliding Mode Technique

Nguyen Anh Tuan *, Ho Pham Huy Anh **

**, ** Ho Chi Minh City University of Technology (HCMUT), 268 Ly Thuong Kiet Street, Dien Hong Ward, Ho Chi Minh City, Viet Nam (nguyenanhtuan.sdh21@hcmut.edu.vn, hphanh@hcmut.edu.vn)*
**, ** Vietnam National University Ho Chi Minh City (VNU-HCM), Tan Lap Quarter, Dong Hoa Ward, Ho Chi Minh City, Viet Nam (nguyenanhtuan.sdh21@hcmut.edu.vn, hphanh@hcmut.edu.vn)*
** Faculty of Engineering and Technology (FET), Sai Gon University (SGU), 273 An Duong Vuong Street, Cho Quan Ward, Ho Chi Minh City, Viet Nam*
(natuan@sgu.edu.vn)
***hphanh@hcmut.edu.vn (Corresponding Author)*

Abstract: This study proposes the novel DANSMC-MDE algorithm for the coupled tank system (CTS) liquid level control, which consists of the Modified Difference Evolution (MDE) method for optimizing parameters of the Direct Adaptive Neuro Sliding Mode Controller (DANSMC). The CTS plant represents a nonlinear object with delay and uncertainties, including varying parameters, sensors, and output valve noises, etc. The suggested controller contains a direct adaptive controller directly approximated by a Radial Basis Function (RBF) neural network combined with a sliding mode controller used to compensate for the approximation errors of the RBF network and to ensure system stability. The Lyapunov stability criterion is used to construct both of the sliding-mode control system and the adaptive rule. Simulations are conducted to demonstrate the effectiveness of the proposed DANSMC-MDE control method. Furthermore, to demonstrate the superiority of the suggested control method, it is contrasted with the optimal SMC and the direct adaptive neuro sliding mode control (DANSMC) approaches.

Keywords: Modified Differential Evolutionary (MDE) method, Direct Adaptive Neuro Sliding Mode Controller (DANSMC), coupled-tank system (CTS), Radial Basis Function neural network (RBFNN).

1. INTRODUCTION

Accurate control of liquid levels between tanks in industrial processes is crucial. Most of these tanks exhibit highly nonlinear characteristics, such as delays between tanks, sensor noise, environmental changes, and interactions among the tanks, etc. The Coupled-Tank System (CTS) shares similar nonlinear behavior with these tanks and is therefore commonly used to validate control algorithms ranging from classical to modern approaches. First, (Fellani and Gabaj, 2015) uses the PID method to control the CTS system. Next, the sliding mode controller (SMC) was proposed in (Saad and Ramadhan, 2019) to improve the control quality of nonlinear objects, where the integral sliding surface was improved to reduce the chattering phenomenon of the traditional SMC. In contrast to existing SMC controllers, the dynamic SMC controller method suggested by (Louis, 2020). (Gouta, 2019) uses a generalized predictive controller as the main controller and an adaptive interconnected high gain observer to observe the system states for controlling the CTS system.

Intelligent control solutions have been widely applied to handle increasingly nonlinear systems. First, the author in (Raj, 2023) uses a Fuzzy PI controller designed using s- and z-type membership functions to address the uncertain environment in the CTS system control, showing improved performance over conventional Fuzzy PI controllers. Neural networks, with their ability to approximate nonlinear systems, were employed in (Sousa et al., 2020) to address the nonlinear behavior of switches along with relations among control parameters in CTS plant regulation. To further improve control performance, numerous studies have coupled NN-fuzzy logic via sophisticated control methods, including sliding or adaptive methods. First is the adaptive fuzzy SMC controller (Zeghlache, 2023), which tackles the issue of external noises and actuator failures. Continually, (Su et al., 2023) suggested an adaptive FSMC algorithm using a modified regressive NN estimator to evaluate the uncertainties of an RM maglev plant. The proposed algorithm applied erroneous values along with perturbations in regulating the RM motor regarding disturbances. The performance is confirmed via quick convergent speed and decreased chatter effect in comparison with other control approaches. Next, (Han and Liu, 2020; Wang, 2021; Li, 2022; Yang, 2022; Chaudhuri, 2020; Fu et al., 2022; Nghia, 2022) employed the Adaptive Neuro Sliding technique. (Han and Liu, 2020) proposed combining SMC and fractional-order neural network methods to address the synchronization issue of fractional-order neuro networks. Meanwhile, (Wang, 2021) used an enhanced state observation technique to lower the level of high-order systems caused by neural networks during approximation. (Li, 2022) uses a hybrid SMC-NN scheme to control a nonlinear SISO system with unknown dynamics. (Yang, 2022) employed a hybrid sliding model-NN control algorithm to approximate the nonlinear characteristics and uncertainties online. (Chaudhuri, 2020; Fu et al., 2022) use an adaptive neural sliding mode controller designed based on a recurrent neural network to ensure optimal tracking performance utilizing the RBF neural network's powerful estimation capabilities, (Nghia, 2022; Zhao and Jin, 2022) suggested using the RBF neural network in conjunction with an adaptive neuro sliding mode controller

(ANSMC) to estimate the model's uncertainties and external perturbations. (Shanmugam and Joo, 2023) applied a hybrid RBFNN-integral ISMC algorithm to regulate the hysteresis of uncertain plants in which RBFNN is used to approximately observe internal/external perturbations, to improve the convergent speed of plants' residual to null. The SMC was then used in order to ensure the system converged. However, trial and error technique is often utilized to choose the controller's parameter values, which results in a significant degree of error in the system response during the initial stage. Calculating and selecting controller parameters for nonlinear systems through trial and error is complex, often time-consuming, and still fails to find optimal parameters in many cases.

Therefore, many studies aim to find controllers' coefficients by utilizing meta-heuristic optimization methods to determine global optimum parameters, even when the fitness function is non-differentiable. Initially, the predicted fuzzy controller is optimized using the PSO technique (Thamallah et al., 2019). Next, the differential evolution (DE) along with techniques using genetic algorithms (Saad, 2012), the improved optimization of ant colonies (m-ACO) method (Chauhan, 2021), and the tree seed optimization (TSO) method (Kr and Mahapatra, 2024) are used to optimize the PID controller parameters for improved control quality. Most meta-heuristic methods are inspired by natural phenomena or the behavior of animals like fish, insects, planets, etc. Due to their advantages and disadvantages, some methods have succeeded, while others are no longer in use. In 2020, RAO introduced an optimization method focused on simplicity and efficiency (Rao, 2020) without relying on natural phenomena or animal behaviors like the methods mentioned above. The quality of optimization methods is often influenced by the parameters chosen, and the strength of the RAO methods is that they only require common control parameters, such as population size and the number of iterations, without needing method-specific control parameters. Taking advantage of the simplicity yet efficiency of this method, (Sahay et al., 2023) applied it to solve the grid dispatch problem's optimization in power flow. The proposed method showed better performance compared to several other optimization methods.

Based on RAO's approach of seeking simple yet effective optimization methods, (Ghasemi, 2023) proposed the FISA, an enhanced approach of RAO method. This study demonstrated that the proposed method achieved better optimization performance than several other optimization methods. Differing from the RAO and FISA methods presented above, the DE method, despite requiring the selection of specific method parameters, remains one of the simplest yet effective meta-heuristic methods. (Wang and Zhang, 2011; Liu and Lampinen, 2005) have analyzed parameter selection and improved method versions for enhanced effectiveness. (Iruthayarajan and Baskar, 2009; Van Kien et al., 2021; Iweh and Akupan 2023) have demonstrated the effectiveness of the DE method over other methods in optimizing controllers for complex nonlinear systems.

Based on the analysis of the above studies, the general trend in control methods is to address model uncertainties and exogenous disturbances to ensure robust and accurate control. In particular, the adaptive neural SMC method with the RBF neural network allows for good approximation of nonlinear uncertainties, combined with the fast convergence characteristic of the SMC method for nonlinear systems, resulting in improved control quality. Additionally, meta-heuristic optimizing techniques contribute to determining the controller's global optimal parameters. These positive aspects have not yet been applied to the Coupled Tank System (CTS). To fill this gap, this study suggests designing and implementing a Direct Adaptive Neuro-SMC (DANSMC) control for liquid-level regulation in the CTS system, with its parameters tuned using the MDE technique. The stability of the system is then ensured by the DANSMC controller, which is constructed based on the Lyapunov theorem.

This paper's major contributions include,

- The new DANSMC control algorithm is innovatively built regardless of specific plant knowledge. It consists of two components: an adaptive control part directly approximated online based on the RBFNN, combined with the adaptive law for removing the approximating errors of the RBFNN. Here, the SMC controller is an additional component that guarantees the system's stable convergence in which uses Lyapunov's stability theorem in the design process for ensuring the system's stability.

- The DANSMC controller's parameters are effectively and initiatively optimized for handling the CTS system using the MDE optimization technique. Here, the MDE method was found to deliver the best performance in comparison with other state-of-the-art meta-heuristic optimization algorithms.

The rest of this study is structured as follows: Section 2 covers the control system presentation. Section 3 introduces the suggested DANSMC-MDE control method. Section 4 illustrates the benchmark test results, and Section 5 concludes the paper.

2. CTS CONTROL SYSTEM PRESENTATION

The CTS model in Figure 1 is an uncertain nonlinear two-DOF system based on the Quanser model, which is a part of the quadruple-tank MIMO system shown in Figure 2.

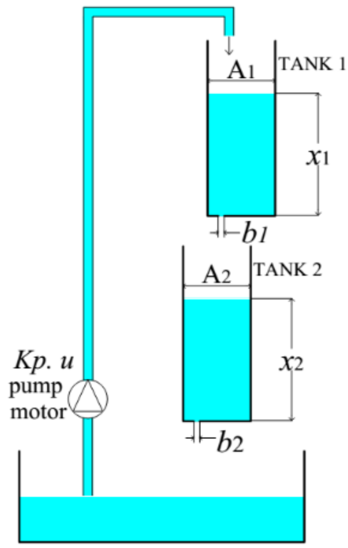

Fig. 1. Coupled tank (CTS) system.

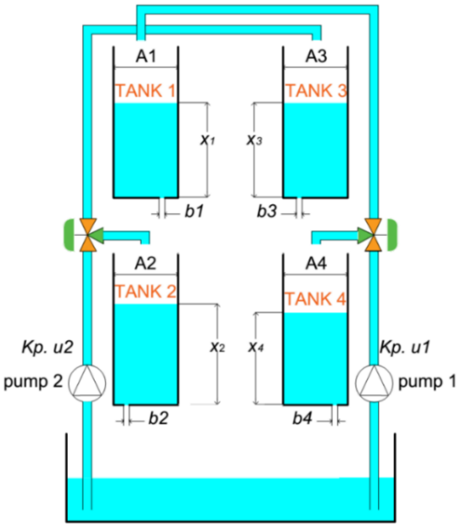

Fig. 2. Quadruple-tank system (QTS).

In the CTS system shown in Figure 1, the voltage input u controls Pump , which supplies liquid directly to Tank 1, while Tank 2 receives liquid from Tank 1. The mathematical model described in (Van Kien et al., 2021) is presented as follows

$$\begin{cases} \dot{x}_1 = \dfrac{1}{A_1}(K_p u - b_1 C_1 \sqrt{2gx_1}) \\ \dot{x}_2 = \dfrac{1}{A_2}(b_1 C_1 \sqrt{2gx_1} - b_2 C_2 \sqrt{2gx_2}) \end{cases} \tag{1}$$

Where, x_1 and x_2 represent the liquid levels in Tank 1 and Tank 2, respectively. The control objective may involve either or both of these variables. In this paper, the control focuses on regulating x_2 . The parameter values of system (1) are provided in Table 1.

Table 1. Parameters of the CTS (1) used for simulation.

Symbol	Elements of the CTS system	Size (unit)
A_1	Surface of tank 1's interior	16.619 (cm^2)
A_2	Surface of tank 2's interior	16.619 (cm^2)
b_1	The drain pipe's cross-sectional area in Tank 1	1 (cm^2)
b_2	The drain pipe's cross-sectional area in Tank 2	1 (cm^2)
C_1	Tank 1 outlet discharge coefficient	0.8
C_2	Tank 2 outlet discharge coefficient	0.8
g	Gravitation force	981 (cm/ s^2)
K_p	Gain of the pump	50 cm^3/(s.V)

3. THE PROPOSED DANSMC-MDE CONTROLLER

3.1 The DANSMC controlling approach and the problem statement

The DANSMC controller for the CTS system (1) is presented as follows.

$$\begin{cases} \dot{x} = f(x) + g(u) \\ y = h(x) \end{cases} \tag{2}$$

Rewrite equation (2) with $h(x) = x_2$

$$\begin{cases} \dot{x}_1 = \dfrac{1}{A_1}(K_p u - \mathrm{b}_1 \mathrm{c}_1 \sqrt{2gx_1}) \\ \dot{x}_2 = \dfrac{1}{A_2}(\mathrm{b}_1 \mathrm{c}_1 \sqrt{2gx_1} - \mathrm{b}_2 \mathrm{c}_2 \sqrt{2gx_2}) \\ y = x_2 \end{cases} \tag{3}$$

Then, equation (3) can be rewritten as follows

$$\ddot{y} = a(x) + b(x)u \tag{4}$$

The task here aims to adjust the output $y(t)$ to follow the predetermined desired value $y_d(t)$. The controller, as determined by the linearized feedback regulations, is

$$u = \frac{1}{b(x)}\left[-a(x) + v(\mathrm{t})\right] \tag{5}$$

Problem 1 formulation:

Where v(t) is the input vector of the system. If the nonlinear functions $a(x)$ and $b(x)$ are known in advance, the control law (5) can be obtained. However, in practice, these functions are often unknown or may vary during operation. In such cases, the control law (5) cannot be directly derived. Therefore, it is necessary to design a control law that allows for online estimation of these functions. To address this issue, we propose the DANSMC controller shown in Figure 3, as follows

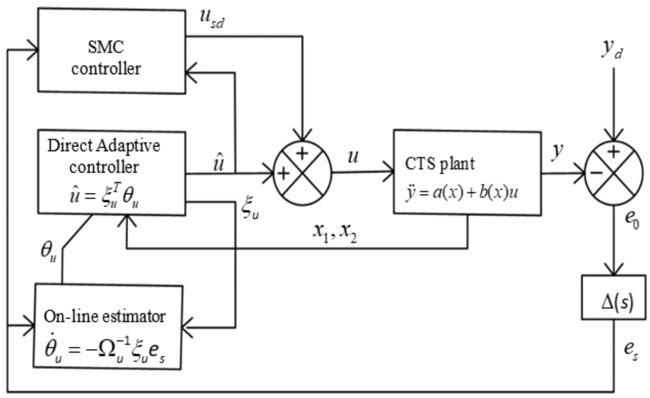

Fig. 3. DANSMC controller diagram for the CTS system.

The DANSMC controller in Figure 3 consists of two components: the sliding control component, which stabilizes the system, and the adaptive control component, which is the main controller and is designed in detail as follows.

The RBFNN approximating control law (5) has two inputs, x_1 and x_2 , nine RBF neurons in the hidden layer, and one output, as shown in Figure 4

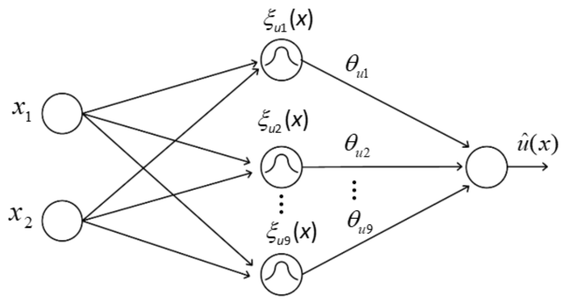

Fig. 4. The RBFNN for approximating the control law (5).

From Figure 4, the Direct Adaptive controller is computed as follows.

$$\hat{u} = \xi_u^T \theta_u \quad (6)$$

With the hidden layer output ξ_u consisting of nine components.

$$\xi_u(x) = [\xi_{u1}(x)\ \xi_{u2}(x)\ ...\ \xi_{u9}(x)]^T \quad (7)$$

The output of the i-th RBF neuron in the hidden layer is calculated as follows.

$$\xi_{ui}(x) = e^{-\frac{\left[(x_1-\mu_{1i})^2+(x_2-\mu_{2i})^2\right]}{2\sigma_i^2}} \quad (8)$$

Design of the RBFNN with RBF neurons evenly distributed in the state space, where the width $\sigma_i = \sigma$

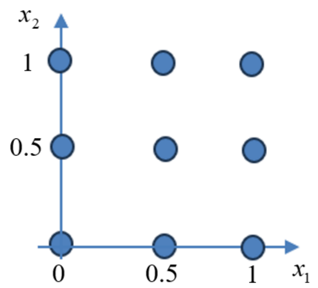

Fig. 5. The center positions of the RBF neural network.

Figure 5 illustrates the distribution of the RBF centers. Using a large number of RBF neurons may slow down the controller's response or exceed the hardware's resource capacity. Conversely, selecting too few neurons may lead to poor approximation performance, making it difficult for the controller to handle varying uncertainties affecting the system, thus degrading control quality. After testing, this study selects 9 RBF neurons.

The vector θ_u represents the output weights of the RBFNN.

$$\theta_u = [\theta_{u1}\ \theta_{u2}\ ...\ \theta_{u9}]^T \quad (9)$$

The RBFNN, with a finite number of RBF neurons, updates the weight vector θ_u online so that $\hat{u}$ approaches the ideal control value u^*. Therefore, a structural approximation error exists as shown in (10).

$$u^*(x) = \theta_u^{*T}\xi_u(x) + \delta_u(x) \quad (10)$$

Therefore, the deviation between the approximated controller and the ideal controller is expressed as follows.

$$\hat{u}(x) - u^*(x) = \tilde{\theta}_u^T \xi_u(x) - \delta_u(x) \quad (11)$$

Where the approximation error $\tilde{\theta}_u$ is defined as follows.

$$\tilde{\theta}_u = \theta_u - \theta_u^* \quad (12)$$

***Assumption* 1**: There always exists an upper bound $\bar{\delta}_u(x)$ for the structural approximation error $\delta_u(x)$, such that $|\delta_u(x)| \le \bar{\delta}_u(x)$, $\forall x$.

Since the structural approximation error $\delta_u(x)$ may cause system instability, a sliding mode control u_{sd} component is added and designed to ensure Lyapunov stability of the system.

$$u = \hat{u} + u_{sd} \quad (13)$$

Based on equation (4), the following expression is derived

$$\ddot{y} = a(x) + b(x)u^*(t) + b(x)\left[u(t) - u^*(t)\right]$$

$$\ddot{y} = v(t) + b(x)\left[u(t) - u^*(t)\right] \quad (14)$$

With $v(t) \in R$ represents the plant dynamics' input vector, which is described as,

$$v(t) = \ddot{y}_d + \bar{e}_s + \eta e_s \quad (15)$$

With $\eta > 0$, e_s and $\bar{e}_s$ are defined as follows

$$e_s(t) = \dot{e}_0(t) + k_1 e_0(t) \quad (16)$$

$$e_0(t) = y_d(t) - y(t) \quad (17)$$

$$\bar{e}_s = \dot{e}_s - \ddot{e}_0 = k_1\dot{e}_0 \quad (18)$$

Whereas the plant's output error is denoted by $e_0(t)$, the tracking error by $e_s(t)$, and parameter k_1 is chosen to meet the Routh-Hurwitz criteria, which are described as $\Delta_s = \dot{s} + k_1 s$

Combining equations (18), (14) - (15) results in:

$$\ddot{e}_0(t) = \ddot{y}_d(t) - \ddot{y}(t) \quad (19)$$

$$\ddot{e}_0(t) = \ddot{y}_d(t) - v(t) - b(x)\left[u(t) - u^*(t)\right] \quad (20)$$

$$\ddot{e}_0(t) = -\bar{e}_s - \eta e_s - b(x)\left[\hat{u}(t) + u_{sd}(t) - u^*(t)\right] \quad (21)$$

When (11) and (18) are substituted into (21), the dynamic features of the tracking error are as follows.

$$\dot{e}_s + \eta e_s = -b\tilde{\theta}_u^T \xi_u(x) + b\delta_u(x) - bu_{sd}$$

Then,

$$\dot{e}_s = -\eta e_s - b\tilde{\theta}_u^T \xi_u(x) + b\delta_u(x) - bu_{sd} \quad (22)$$

Selecting a quadratic Lyapunov candidate as,

$$V = \frac{1}{2b}e_s^2 + \frac{1}{2}\tilde{\theta}_u^T Q_u \tilde{\theta}_u \tag{23}$$

In which Q_u being a positive constant.

Assumption 2: $b(x)$ consistently stay inside a bounded range

$0 < \underline{b}(x) \le b(x) \le \overline{b}(x) < \infty$

Taking the time derivative of V, it yields.

$$\dot{V} = \frac{1}{b}e_s\dot{e}_s - \frac{\dot{b}}{2b^2}e_s^2 + \tilde{\theta}_u^T Q_u \dot{\theta}_u \tag{24}$$

When (22) is inserted into $\dot{V}$, it gives,

$$\dot{V} = -\frac{\eta e_s^2}{b} - e_s\tilde{\theta}_u^T\xi_u + e_s\delta_u - e_s u_{sd} - \frac{\dot{b}}{2b^2}e_s^2 + \tilde{\theta}_u^T Q_u \dot{\theta}_u$$

Then,

$$\dot{V} = -\frac{\eta e_s^2}{b} - e_s u_{sd} + e_s\delta_u + \tilde{\theta}_u^T(Q_u\dot{\theta}_u - \xi_u e_s) - \frac{\dot{b}}{2b^2}e_s^2 \tag{25}$$

The adaptation law is chosen as follows

$$\dot{\theta}_u = Q_u^{-1}\xi_u e_s \tag{26}$$

Taking (26) into (25), we obtain

$$\dot{V} = -\frac{\eta e_s^2}{b} - e_s u_{sd} + e_s\delta_u - \frac{\dot{b}}{2b^2}e_s^2$$

$$\dot{V} \le -\frac{\eta e_s^2}{b} - e_s u_{sd} + |e_s|(|\delta_u| + \frac{|\dot{b}|}{2b^2}|e_s|)$$

$$\dot{V} \le -\frac{\eta e_s^2}{\overline{b}} - e_s u_{sd} + |e_s|(\overline{\delta}_u + \frac{\gamma_b}{2\underline{b}^2}|e_s|) \tag{27}$$

Assumption 3: It exists a well-defined function $\gamma_b(x)$ such that $|\dot{b}|(x) \le \gamma_b(x)$

Then the sliding control component is selected as follows.

$$u_{sd} = (\overline{\delta}_u + \frac{\gamma_b}{2\underline{b}^2}|e_s|)\,\mathrm{sgn}(e_s) \tag{28}$$

Replacing (28) into (27), we obtain

$$\dot{V} \le -\frac{\eta e_s^2}{\overline{b}} \le 0 \tag{29}$$

Because V is a non-negative definite function and its time derivative $\dot{V} \le 0$, the proposed DANSMC controller ensures Lyapunov stability for the system

Problem 2 formulation:

Finding the optimal values for the parameters σ_i, k_1, and Q_u in equations (8), (16), and (26), through a trial-and-error technique is very challenging. Therefore, this paper proposes an optimization algorithm to tune these parameters, as described in the following sections.

3.2 Assessment of optimization algorithms for tuning the DANSMC controller parameters in the CTS system

Five optimization algorithms PSO in (Thamallah, 2019), GA in (Saad, 2012), Rao 3 in (Rao, 2020), FISA in (Ghasemi, 2023), and MDE in (Son, 2020) are used to optimize the DANSMC controller. All of these algorithms have a similar initiated requirement regarding the fitness equation (30). Every algorithm is run ten times from the same starting point of fitness value as to ensure an equal comparison. The convergence values of these met

hods are then compared using the average results from these ten runs.

Table 2. Five optimization algorithms' parameters.

Method	Parameters	Value
General	Population size, NP	50
	Number of generations,	300
	Four variables' upper bound, [k_1, η, σ^2, Q_u^{-1}]	[50, 20, 20, 100]
	Four variables' lower bound	[0.01, 0.01, 0.01, 1]
	Initial fitness function value	13.552
PSO	Velocity update constant c_1, c_2	2
	Inertia weight	0.4
GA	Mutation rate	10%
	Crossover rate	90%
	Stall generation	200
	Tolerance for convergence functions	10^{-3}
RAO 3	No particular method parameters	
FISA	No particular method parameters	
MDE	Mutation coefficient, F	[0.4, 1]
	Crossover rate, CR	[0.7, 1]

Table 2 illustrates the parameters of the five optimization algorithms: PSO, GA, RAO-3, FISA, and MDE. These parameters include both standard and algorithm-specific data. An incorrect choice of these parameters could have a negative impact on the quality of convergence. When tuning the controller parameters for the CTS system (1), under the physical constraints of the system, such as the control input voltage $u \in [0, 24]$ V and the state variables x_1, $x_2 \in [0, 30]$ cm, the parameters listed in this table, after testing, provide the best convergence of the fitness function for the considered optimization algorithms.

Based on the ISE criterion assessed for 350 seconds, the following fitness function is selected and applied to all five algorithms.

Fitness function

$$f = \int_0^t e_0^2(t)dt \tag{30}$$

with $e_0 = (y_d - y)$ from (17).

First, the initial value of the fitness function was generated using the PSO algorithm, yielding a result of $f_0 = 9.8759$. Next, all optimization algorithms were executed starting from this initial objective value.

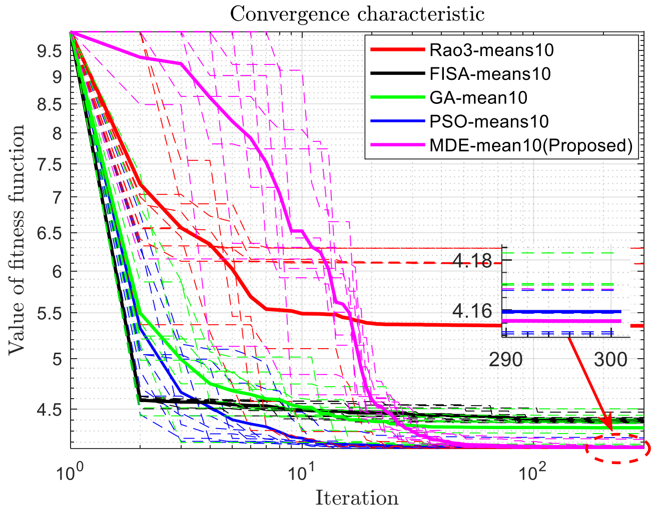

Fig. 6. Comparative fitness functions for DANSMC's parameters optimization.

The comparison results of parameters that were optimally tuned for the DANSMC controller are shown in Figure 6, where the RAO 3 technique yielded the maximum convergence and the MDE technique the lowest. As explained in the next sections, this study proposes employing the MDE optimization technique to optimally fine-tune the DANSMC's parameters.

3.3 Suggested DE Method

(Van Kien et al., 2021) proposed the DE method for finding the global optimum of fitness functions. The following is a summary of the method.

Initializing stage

To initiate the DE technique, a random starting population of NP individuals is created, each represented as a D-sized vector.

$$\vec{X}_{i,G} = (x_{1,i,G}, x_{2,i,G}, \ldots, x_{D,i,G}) \tag{31}$$

With D variables constrained by x_{Min}, x_{Max}, each individual reflects the optimum result. G represents the number of evolutionary iterations, $G = 0,1,2\ldots,G_{Max}$, $i = 1,2,\ldots, NP$.

Mutating stage

Three distinct vectors $\vec{X}_{r_1^i}$, $\vec{X}_{r_2^i}$, $\vec{X}_{r_3^i}$ from the current iteration population are randomly combined to form the goal vector for the i-th individual.

$$\vec{V}_{i,G} = \vec{X}_{r_1^i,G} + F(\vec{X}_{r_2^i,G} - \vec{X}_{r_3^i,G}) \tag{32}$$

The randomized integers r_1^i, r_2^i, r_3^i in this case must be different from the goal vector and fall within $[1, NP]$. Amongst 2 of 3 vectors, the modified factor $F \in [0,1]$ lessens the difference.

Cross-over stage

Following the creation of the goal vector, the crossover operation is performed to increase the variation within the population. The mutated vector $\vec{V}_{i,G}$ is crossed with $\vec{X}_{i,G}$ to create a test vector $\vec{U}_{i,G} = [u_{1,i,G}, u_{2,i,G}, \ldots, u_{3,i,G}]$. Typically, the DE method is used to build the testing vector using a binomial crossover strategy, which is described as follows.

$$u_{j,i,G} = \begin{cases} v_{j,i,G} & \text{if } (\text{rand}_{j,i}[0,1] \le CR) \\ x_{j,i,G} & \text{otherwise} \end{cases} \tag{33}$$

With $i = 1,2,\ldots, NP$; $j = 1,2,\ldots, D$; CR is a random number that represents the Crossing Ratio.

Selection stage

An evaluation is done between the target vector $\vec{X}_{i,G}$ and trial one $\vec{U}_{i,G}$. The selecting process is described as follows.

$$\vec{X}_{i,G+1} = \begin{cases} \vec{U}_{i,G} & \text{if } f(\vec{U}_{i,G}) \le f(\vec{X}_{i,G}) \\ \vec{X}_{i,G} & \end{cases} \tag{34}$$

Here, $f(\vec{X})$ denotes the fitness equation.

Converging stage

Every iteration goes through all of the stages-mutation, crossover, and selection-and is repeated until one of the following conditions is met: the number of iterations reaches its maximum, the fitness function achieves the desired minimum value, or it remains unchanged for a specified period.

3.4 Optimal tuning of the DANSMC controller parameters using the proposed MDE technique

The mutation coefficient F and the crossover rate CR play a crucial role in the performance of the algorithm; if not properly selected, they can significantly affect the algorithm's quality. Therefore (Son, 2020) proposed the Modified Differential Evolution (MDE) algorithm in which F and CR are not fixed as in the basic DE algorithm (Van Kien et al., 2021) but instead vary randomly after each generation with values of $F \in [0.4,1]$ and $CR \in [0.7,1]$. This study demonstrated that the MDE algorithm provides better optimal solution quality than the basic DE algorithm, as shown in the fitness function comparison graphs. Leveraging the strength of this algorithm, this study suggests the use of the MDE method where F and CR are not fixed but change randomly after each generation with $F \in [0.4,1]$ and $CR \in [0.7,1]$, in order to enhance the quality of the optimal solution.

Fig. 7 shows the DANSMC controller structure with the MDE method-optimized parameters. Np = 50 individuals, D = 4 variables, and $G_{Max} = 300$ generations are used to determine the population size. These three variables' bounds are shown in Table 3.

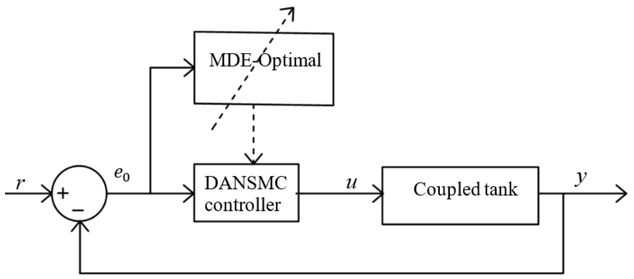

Fig. 7. DANSMC parameters are optimally estimated using the MDE method.

Table 3. The selection variables' limit boundaries.

Symbols	k_1	σ^2	Q_u^{-1}
x_{Min}	0.01	0.01	1
x_{Max}	50	20	100

Figure 8 shows the graph of the comparative fitness function after ten optimization runs of the DANSMC's parameters over 300 generations, showing a consistent decrease in the fitness function. After approximately 200 generations, all runs converge, with their fitness values stabilizing around 4.14. This demonstrates the convergence capability of the proposed MDE method in optimally identifying the DANSMC's coefficients.

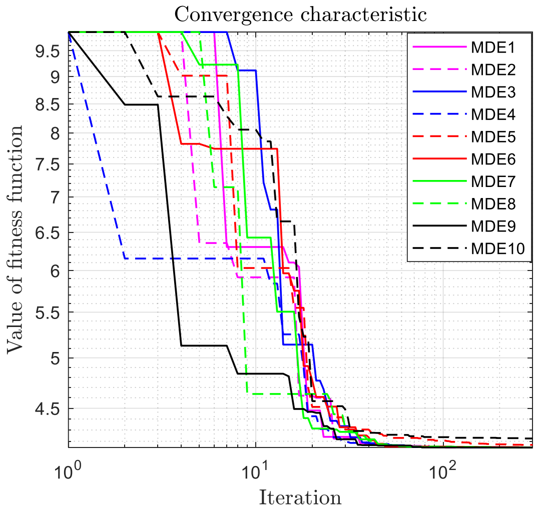

Fig. 8. Comparative fitness function while employing the MDE method to optimize DANSMC's parameters.

Among runs, the first run, represented by the MDE1 curve, achieved the lowest convergence value of 4.14539. When the fitness function (3.30) reaches its minimum, the error *e* also reaches its minimum. As a result, the numerical simulation in Section 4 will use the solution from this run, which is found in the following table.

Table 4. Resulted values of decision variables.

	Decision variables		
Resulted X	k_1	σ^2	Q_u^{-1}
Value	0.01	16.2366	23.4756

4. SIMULATION RESULTS

The simulation of the proposed DANSMC-MDE control system is carried out using the optimum coefficients of the DANSMC control system optimized by the MDE method introduced in Subsection 3.4 for controlling the CTS plant. Here, the comparative performance is carried on between the DANSMC with SMC-MDE and the SMC method in (Saad and Ramadhan, 2019), which were also parameter optimized using the MDE method with the identical optimization settings as the DANSMC control system.

The conventional SMC controller in (Saad and Ramadhan, 2019) can be easily reconstructed for system (1) as follows.

Select the sliding surface for the second-order system as: $S = \dot{e}_0 + ke_0$, then $\dot{S} = \ddot{e}_0 + k\dot{e}_0$; where $e_0 = y_d - y$, then $\ddot{e}_0 = \ddot{y}_d - \ddot{y}$. Choose $\dot{S} = -Ksign(S)$. Based on these expressions and Equation (5), the conventional SMC control law for the CTS system (1) is obtained as follows.

$$u_{SMC} = \frac{1}{b(x)}\left[-a(x) + \ddot{y}_d + k\dot{e}_0 + Ksign(S)\right] \tag{35}$$

The sign function in equation (35) is replaced by the saturation function to mitigate the chattering effect. Optimal tuning was performed using the MDE algorithm described in Section 3.4 over 300 generations and 10 runs, with k constrained to the range [0, 100] and K to [0, 60]. The resulting optimal values of k and K are: $k = 99.6838$, $K = 59.9424$.

- **The 1st Benchmark test**: Comparison of the control methods in response to a trained and varying reference signal. Figure 9 shows the output tracking performance of each approach under a trained and varying reference signal, except for the SMC-MDE method, which exhibits oscillatory behavior around the benchmark when the reference signal changes.

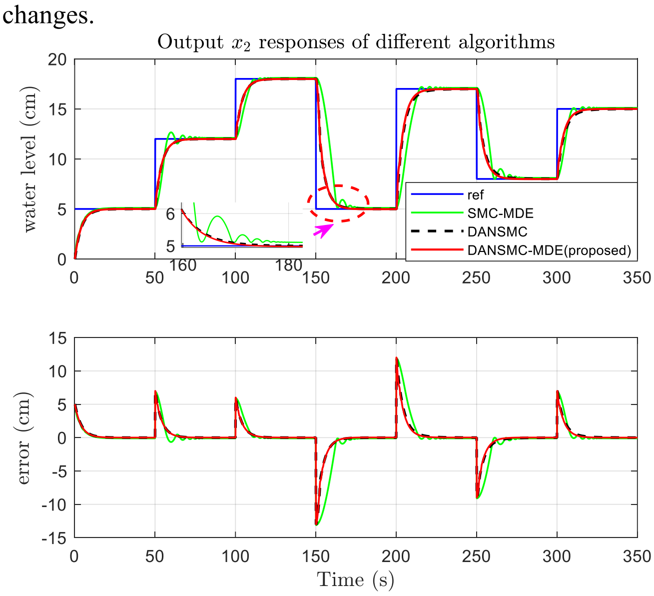

Fig. 9. Output response of the CTS system under various control strategies to the trained reference signal.

The DANSMC-MDE method achieves the fastest response, reaching steady state in approximately 20 seconds, with zero steady-state error and no overshoot.

Furthermore, the performance of the control methods is presented in Table 5, showing that the DANSMC-MDE method provides better response quality than the other approaches.

Table 5. Evaluation of control quality indexes across different comparative algorithms.

	Proposed DANSMC-MDE	DANSMC	SMC-MDE
IAE	**239.8**	268.8	395.5
ISE	**1163**	1397	2666
ITAE	**$4.02*10^4$**	$4.418*10^4$	$6.991*10^4$

- **The 2nd Benchmark test**: Comparison of the control methods in response to an untrained and varying reference signal.

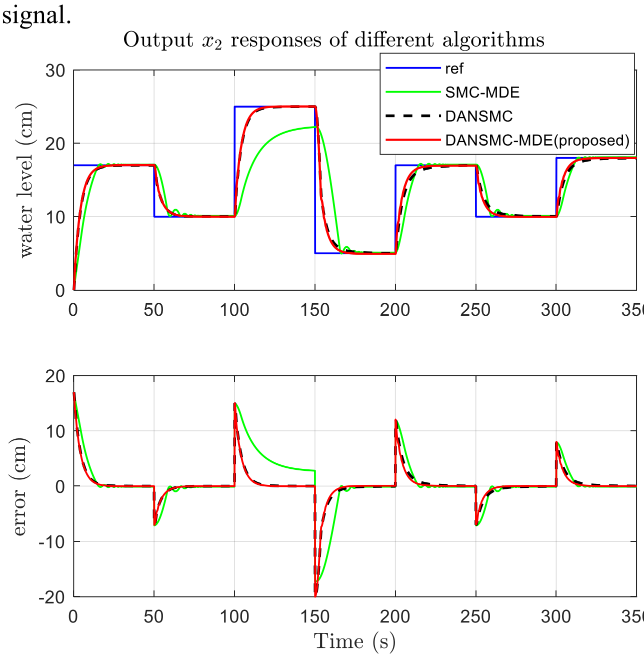

Fig. 10. Output response x_2 of the CTS system to an untrained reference signal.

Fig. 10 presents a comparison of responding liquid levels between the proposed DANSMC-MDE with the two other advanced DANSMC and SMC-MDE methods. The DANSMC-MDE method provides a fast response, with no overshooting, and has zero steady-state error even when the reference signal fluctuates more than the trained signal. In the meantime, the SMC-MDE approach shows an undershoot response within 100 and 150 seconds.

- **The 3rd Benchmark test**: Comparison of control methods under an untrained reference signal, sensor noise, and varying model parameters via outlet valve area b_2 disturbance in Tank 2.

Figure 11 demonstrates that from 300 seconds onward, the ANSMC-MDE and ANSMC methods continue to track the reference signal and maintain stability effectively. In contrast, the SMC-MDE method fails to provide satisfactory performance. This degradation is attributed to the conventional SMC's strong dependency on model parameters; hence, when these parameters experience significant variations, the controller's ability to maintain control quality is compromised.

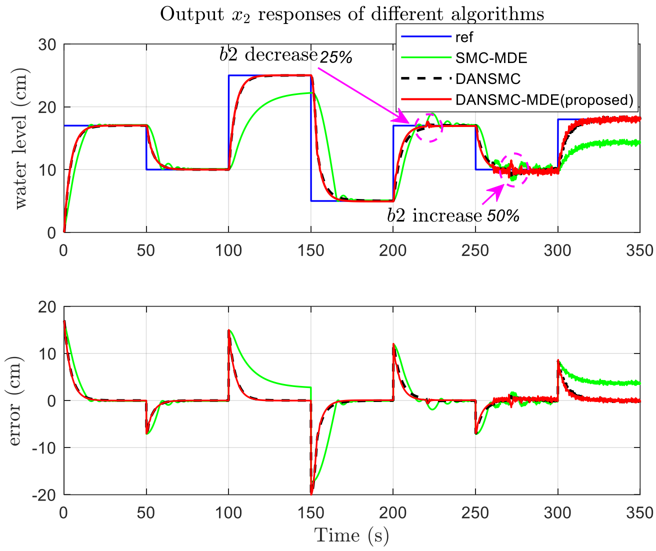

Fig. 11. Output response x_2 of the CTS system to output sensor noise and disturbance drain b_2 with an untrained reference signal.

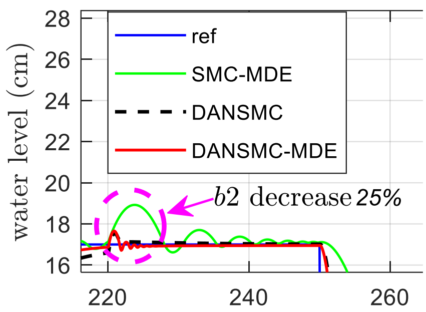

Fig.12. The CTS system output response to output sensor noise and decreases drain with untrained reference signal (zooming from Fig. 11).

Figures 12 and 13 show a 25% reduction in the outlet valve area of Tank 2 from 220 seconds and a 50% increase from 270 seconds. In Figure 12, the DANSMC-MDE and DANSMC methods exhibit brief overshoots lasting approximately 1.5 seconds before stabilizing, while the SMC-MDE method shows a significant overshoot occurring after 220 seconds. Figure 13 shows the presence of output sensor noise with a variance of 0.05 and a mean of 0. Starting from 260 seconds onward, the ANSMC-MDE and ANSMC methods maintain stable responses oscillating around the reference signal. Furthermore, when the outlet valve is disturbed with a 50% increase from 270 seconds onward, the output exhibits increased oscillations but remains stable after approximately 3 seconds.

Figure 14 illustrates the responses of the nine output weights θ_u in the RBFNN of the DANSMC-MDE controller under output sensor noise and disturbances in Tank 2's drain, using an untrained reference signal. The results indicate that the weights adapt swiftly, enabling the controller to maintain the system stability and ensure accurate tracking performance despite variations in the reference signal, sensor noise, and system parameters.

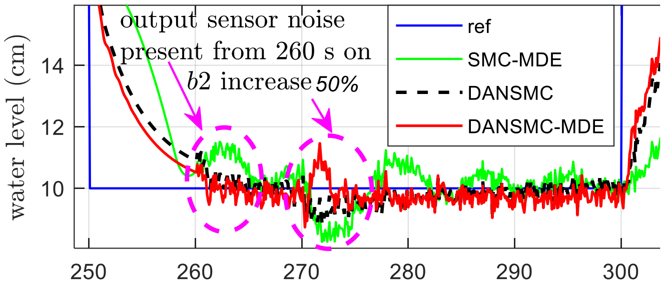

Fig. 13. The CTS system output response to output sensor noise and increases drain with untrained reference signal (zooming from Fig. 11).

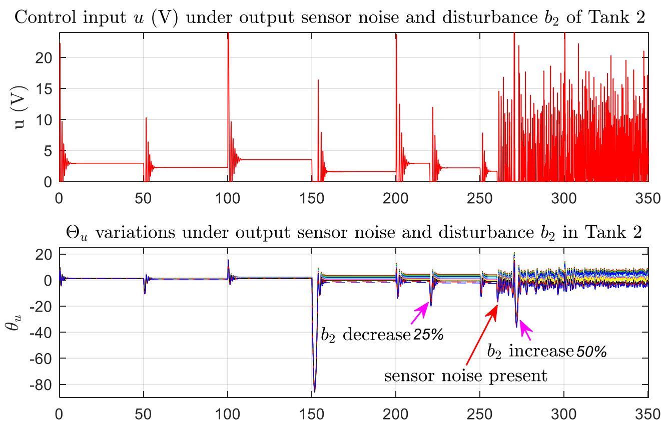

Fig. 14. CTS system output x_2 response to output sensor noise and disturbance drain b_2 of Tank 2 with an untrained reference.

The above results demonstrate that the proposed DANSMC-MDE algorithm delivers superior response quality compared to other methods, as validated using both trained and untrained reference signals, as shown in Figures 9 and 10. Additionally, evaluations under output sensor noise and model parameter disturbances highlight the controller's effective online adaptability, as illustrated in Figures 11 through 14.

The mathematical model of the controlled system is necessary for the conventional SMC algorithm to function. Consequently, the system becomes unstable when the reference signal varies and the model parameters change significantly. In contrast, the DANSMC algorithm and the proposed method are designed without relying on the mathematical model of the plant, instead utilizing the fast and effective approximation capability of the RBF neural network (RBFNN). Additionally, the proposed algorithm is developed based on the Lyapunov stability criteria, for ensuring system stability in the presence of uncertainties and external disturbances. However, if the output sensor noise or output drain is intentionally largely disturbed, the current parameters of the proposed controller may no longer be effective. In such cases, it is necessary to adjust the variables' lower and upper bounds or modify other parameters of the optimization algorithms listed in Table 2 to identify new optimal controller parameters and to maintain control performance.

5. CONCLUSIONS

The novel DANSMC-MDE method for CTS system liquid level control is suggested in this study. The proposed method applies the DANSMC method in which its coefficients are optimally identified by the MDE optimization method. The DANSMC controller was designed using the Lyapunov stability theorem to guarantee system stability. To demonstrate the effectiveness and superiority of the proposed method, benchmark tests were conducted comparing it with two other advanced DANSMC and traditional SMC control systems. Benchmark-test results indicate that the proposed technique yields a fast output response without steady-state inaccuracy or overshoot. In particular, most control quality indices perform superior compared to the results of other comparative control methods. Furthermore, regardless of previous training, the system output responds well to significant variations in the reference signal. In addition, the findings confirmed with different model parameters and output sensor noise clearly verify the proposed controller's superior adaptive capability.

Consequently, the proposed DANSMC-MDE approach demonstrates its effectiveness in controlling a variety of highly nonlinear MISO and MIMO systems.

ACKNOWLEDGEMENTS

We acknowledge Ho Chi Minh City University of Technology (HCMUT) and VNU-HCM for supporting this study.

REFERENCES

Chaudhuri, S., et al. (2020). Adaptive neural-bias-sliding mode control of rugged electrohydraulic system motion by recurrent Hermite neural network. *Control Engineering Practice*, 103, 104588.

Chauhan, S., Singh, B., and Singh, M. (2021). Modified ant colony optimization based PID controller design for coupled tank system. *Engineering Research Express*, 3(4), 045005.

Fellani, M.A. and Gabaj, A.M. (2015). PID controller design for two tanks liquid level control system using Matlab. *International Journal of Electrical and Computer Engineering*, 5(3), 436.

Fu, J., Huang, F., and Chen, Z. (2022). Optimization-based adaptive neural sliding mode control for nonlinear systems with fast and accurate response under state and input constraints. *Journal of the Franklin Institute*, 359(13), 6735-6758.

Ghasemi, M., et al. (2023). A new metaphor-less simple algorithm based on Rao algorithms: a Fully Informed Search Algorithm (FISA). *PeerJ Computer Science*, 9, e1431.

Gouta, H., et al. (2019). Experimental sensorless control for a coupled two-tank system using high gain adaptive observer and nonlinear generalized predictive strategy. *ISA Transactions*, 87, 187-199.

Han, Z., Li, S., and Liu, H. (2020). Composite learning sliding mode synchronization of chaotic fractional-order neural networks. *Journal of Advanced Research*, 25, 87-96.

Iruthayarajan, M.W. and Baskar, S. (2009). Evolutionary algorithms based design of multivariable PID controller. *Expert Systems with Applications*, 36(5), 9159-9167.

Iweh, C.D. and Akupan, E.R. (2023). Control and optimization of a hybrid solar PV–Hydro power system for off-grid applications using particle swarm optimization (PSO) and differential evolution (DE). *Energy Reports*, 10, 4253-4270.

Kr, A.G. and Mahapatra, S. (2024). Improving precision and robustness in level control of coupled tank systems: a tree seed optimization and μ-analysis approach. *Results in Control and Optimization*, 15, 100410.

Li, B., et al. (2022). Adaptive neural network sliding mode control for a class of SISO nonlinear systems. *Mathematics*, 10(7), 1182.

Liu, J. and Lampinen, J. (2005). A fuzzy adaptive differential evolution algorithm. *Soft Computing*, 9, 448-462.

Louis, M.A., et al. (2020). Performance investigation and control parameters choice for sliding mode control of coupled tanks system. *IOP Conference Series: Materials Science and Engineering* 973.

Nghia, V.B.V., et al. (2022). Adaptive neural sliding mode control for two-wheel self-balancing robot. *International Journal of Dynamics and Control*, 10(3), 771-784.

Raj, R., et al. (2023). TS fuzzy controller with s-and z-type MFs to control a coupled-tank system. *Materials Today: Proceedings*, 80, A8-A13.

Rao, R.V. (2020). Rao algorithms: Three metaphor-less simple algorithms for solving optimization problems. *International Journal of Industrial Engineering Computations*, 11(1), 107-130.

Saad, M. and Ramadhan, A. (2019). Sliding mode control of nonlinear coupled tank system. *WSEAS Transactions on Systems*, 18, 35-44.

Saad, M.S., Jamaluddin, H., and Darus, I.Z.M. (2012). PID controller tuning using evolutionary algorithms. *WSEAS Transactions on Systems and Control*, 7(4), 139-149.

Sahay, S., Upputuri, R., and Kumar, N. (2023). Optimal power flow-based approach for grid dispatch problems through Rao algorithms. *Journal of Engineering Research*, 11(2), 100032.

Shanmugam, L. and Joo, Y.H. (2023). Adaptive neural networks-based integral sliding mode control for TS fuzzy model of delayed nonlinear systems. *Applied Mathematics and Computation*, 450, 127983.

Son, N.N. (2020). Level control of quadruple tank system based on adaptive inverse evolutionary neural controller. *International Journal of Control, Automation and Systems*, 18(9), 2386–2397.

Sousa, B.S., Silva, F.V., and Fileti, A.M.F. (2020). Level control of coupled tank system based on neural network techniques. *Chemical Product and Process Modeling*, 15(3), 20190086.

Su, X., Yang, X., and Xu, Y. (2023). Fuzzy adaptive terminal sliding mode control based on recurrent neural network compensation for a maglev system. *Engineering Applications of Artificial Intelligence*, 124, 106588.

Thamallah, A., Sakly, A., and M'Sahli, F. (2019). A new constrained PSO for fuzzy predictive control of Quadruple-Tank process. *Measurement*, 136, 93-104.

Van Kien, C., Anh, H.P.H., and Son, N.N. (2021). Adaptive inverse multilayer fuzzy control for uncertain nonlinear system optimizing with differential evolution algorithm. *Applied Intelligence*, 51(1), 527-548.

Wang, J., et al. (2021). An adaptive neural sliding mode control with ESO for uncertain nonlinear systems. *International Journal of Control, Automation and Systems*, 19, 687-697.

Wang, Y., Cai, Z., and Zhang, Q. (2011). Differential evolution with composite trial vector generation strategies and control parameters. *IEEE Transactions on Evolutionary Computation*, 15(1), 55-66.

Yang, M., et al. (2022). Adaptive neural network-based sliding mode control for a hydraulic rotary drive joint. *Computers and Electrical Engineering*, 102, 108189.

Zeghlache, S., et al. (2023). Adaptive fuzzy fast terminal sliding mode control for inverted pendulum-cart system with actuator faults. *Mathematics and Computers in Simulation*, 210, 207-234.

Zhao, Z. and Jin, X. (2022). Adaptive neural network-based sliding mode tracking control for agricultural quadrotor with variable payload. *Computers and Electrical Engineering*, 103, 108336.